THE JOURNAL OF BIOLOGICAL CHEMISTRY VOL. 282, NO. 50, pp. 36543–36551, DECEMBER 14, 2007

Regulation of Iron Homeostasis Mediated by the Heme-binding Protein Dap1 (Damage Resistance Protein 1) via the P450 Protein Erg11/Cyp51*[S]

Received for publication, August 14, 2007, and in revised form, October 22, 2007 Published, JBC Papers in Press, October 22, 2007, DOI 10.1074/jbc.M706770200

Rolf J. Craven[‡1], **Julia C. Mallory**[‡], **and Randal A. Hand**[§]

From the [‡]*Department of Molecular and Biomedical Pharmacology, University of Kentucky, Lexington, Kentucky 40536 and the* [§]*Department of Pharmacology, University of North Carolina, Chapel Hill, North Carolina 27599*

Fungal infections arise frequently in immunocompromised patients, and sterol synthesis is a primary pathway targeted by antifungal drugs. In particular, the P450 protein Erg11/Cyp51 catalyzes a critical step in ergosterol synthesis, and the azole class of antifungal drugs inhibits Erg11. Dap1 is a heme-binding protein related to cytochrome b_5 that activates Erg11, so that cells lacking Dap1 accumulate the Erg11 substrate and are hypersensitive to Erg11 inhibitors. Heme binding by Dap1 is crucial for its function, and point mutants in its heme-binding domain render Dap1 inactive for sterol biosynthesis and DNA damage resistance. Like Dap1, the human homologue, PGRMC1/Hpr6, also regulates sterol synthesis and DNA damage resistance. In the present study, we demonstrate that the Dap1 heme-1 domain is required for growth under conditions of low iron availability. Loss of Dap1 is suppressed by elevated levels of Erg11 but not by increased heme biosynthesis. Dap1 localizes to punctate cytoplasmic structures that co-fractionate with endosomes, and Dap1 contributes to the integrity of the vacuole. The results suggest that *Saccharomyces cerevisiae* Dap1 stimulates a P450-catalyzed step in sterol synthesis via a distinct localization from its homologues in *Schizosaccharomyces pombe* and mammals and that this function regulates iron metabolism.

Fungal infections are important clinically because they contribute to the mortality of patients with human immunodeficiency virus/AIDS, cancer, and other diseases associated with immunosuppression. Mammalian hosts combat fungal infections via the immune system and by sequestering free iron in the bloodstream. Fungal infections can be suppressed with the azole group of antifungal drugs, a commercially important group of drugs that includes fluconazole, itraconazole, and miconazole. These drugs inhibit Erg11/Cyp51/lanosterol demethylase (1, 2), which catalyzes a critical step in the synthesis of ergosterol, a key component of the fungal cell membrane. Erg11 is one of a large class of monooxygenases that are called P450 proteins due to the spectral absorbance of a cysteine-linked heme molecule in their active site (3).

In *Saccharomyces cerevisiae*, Erg11 is activated by Dap1 (damage resistance protein 1) (4), which is related to cytochrome b_5 (5), a heme-binding protein that activates P450 reactions (3, 6). Cells lacking Dap1 partially arrest sterol synthesis at the stage catalyzed by Erg11 (4), and *dap1*Δ cells are hypersensitive to the Erg11 inhibitors itraconazole and fluconazole (4). According to microarray databases, *DAP1* expression is induced by azole antifungal drugs (7), but this has not been independently confirmed. Azole sensitivity in *dap1*Δ cells is suppressed by overexpressing Erg11 (8), and *dap1*Δ cells have ~4-fold lower levels of Erg11 than wild-type cells (8), although this regulation occurs primarily at the post-transcriptional level. Notably, the effect of Dap1 on sterol synthesis is conserved with its human homologue (9), called PGRMC1 (for progesterone receptor membrane component 1) or Hpr6 (for heme-1 domain protein/human progesterone receptor) (10).

Dap1 binds to heme (8, 11), as does its homologues in *Schizisaccharomyces pombe*, mice, and humans (9, 12, 13). The heme-binding activity of Dap1 is critical for its function, and heme-binding defective mutants are inactive in sterol synthesis or damage resistance (8). Furthermore, the damage sensitivity and sterol synthesis phenotypes of *dap1*Δ mutants can be suppressed by adding exogenous heme (8), suggesting a role for Dap1 in maintaining heme metabolism. One appealing model for Dap1 family proteins is that they utilize their heme-binding activity to directly activate P450 proteins. However, unlike cytochromes and related proteins, Dap1 homologues lack the histidine residues that coordinate heme binding in cytochrome b_5 (5), suggesting that Dap1 may participate in intracellular heme trafficking. In addition to regulating ergosterol synthesis, Dap1 is required for resistance to the alkylating agent methyl methanesulfonate, and *dap1*Δ cells have decreased mitochondrial function (4).

Heme (iron protoporphyrin IX) is synthesized in an eight-step pathway that is subject to regulation at various steps (14). Two key steps in heme synthesis are catalyzed by Hem1/5-aminolevulinate synthase, a mitochondrial protein, and Hem2/δ-aminolevulinate dehydratase/porphobilinogen synthase, which localizes to the cytoplasm and nucleus. Heme and ergosterol share the same upstream precursors (15), and the synthesis of heme and ergosterol are closely synchronized. The Hap1 transcription factor (16) is directly regulated by heme through a series of heme-regulated sequence motifs that control multi-

* This work was supported in part by American Cancer Society Grant 85-001-19-IRG and by National Institutes of Health Grant COBRE P20 RR 15592. The costs of publication of this article were defrayed in part by the payment of page charges. This article must therefore be hereby marked "*advertisement*" in accordance with 18 U.S.C. Section 1734 solely to indicate this fact.

[S] The on-line version of this article (available at http://www.jbc.org) contains supplemental Figs. 1–3.

[1] To whom correspondence should be addressed. Tel.: 859-323-3832; Fax: 859-257-9608; E-mail: rolf.craven@uky.edu.

protein complex formation and DNA binding (17). Heme is also required for the transcription of iron transport and sterol synthetic genes (18). Iron levels, in turn, regulate the transcription, post-transcriptional stability, and post-translational levels of numerous genes and gene products (19–21). One of the iron-regulated transcripts is *DAP1*, which is post-transcriptionally regulated by proteins that respond to low iron conditions (19).

Because of the close relationship between iron metabolism and the synthesis of heme and ergosterol, we have examined the role of Dap1 in these processes. We have found that Dap1 regulates growth under low iron conditions through a mechanism that requires its heme-1 domain, and Dap1-mediated growth on low iron is mediated by Erg11. We have also shown that Dap1 localizes to endosomes and regulates the structure of the vacuole, which is characteristic of other sterol biosynthetic proteins. The results represent a novel function for the Dap1 family proteins, which include homologues in mammals that are important for sterol synthesis and in cancer.

EXPERIMENTAL PROCEDURES

Yeast Strains and Growth Conditions—All strains were isogenic with W303 (*leu2-3,112 his3-11,15 ura3-1 ade2-1 trp1-1 can1-100 rad5-535*) (22). The *rad5-535* allele was replaced with the wild-type *RAD5* gene by crossing and tested by PCR as described (23). Cells were maintained yeast-peptone-dextrose (YPD)[2] or synthetic dextrose plates. Methyl methanesulfonate (Sigma) and bathophenanthroline disulfonic acid (Fisher) were added to plates at the indicated doses. For expression studies, log phase cultures were treated with itraconazole, methyl methanesulfonate, or hydroxyurea (all from Sigma) at the indicated doses.

The strains RCY409-2a (*DAP1*) and RCY409-4b (*dap1*Δ::*LEU2*) and the RCY409-2a and RCY409-4b derivatives harboring the control (pRS313, YEp*lac*181, or YEp*lac*195), *DAP1* (pRC41), *DAP1*-D91G (pRC39), or *ERG11* (pRH4) plasmids have been described previously (8). The pSCCC1 plasmid has also been described previously (24). The *dap1*Δ::*HIS3* strain RCY456 was constructed by one-step transplacement of the entire *DAP1* gene with a PCR product containing *HIS3* and *DAP1*-flanking homology. Oligonucleotide sequences are available as supplemental Fig. 1. For Dap1 expression studies, the *DAP1* open reading frame was fused in frame with three copies of the HA epitope tag sequence by one-step integration of the epitope tag fused to the *KanMX* reporter gene. The HA tag sequence was amplified by PCR with the primers *DAP1*-TAGF and *DAP1*-TAGR, using the plasmid pFA6a-3HA-KanMX6 (25) as a template. W303a cells were transformed with the resulting PCR product, and Geneticin-resistant isolates were tested for insertion of the epitope tag by PCR.

The resulting strain, RCY172, was crossed to the strain RCY308-7b (α *mec1-21 CAN1 RAD5*) (26), and the resulting diploid strain, RCY408, was sporulated and dissected, yielding the wild-type progeny RCY408-1d (α *DAP1 CAN1 RAD5*) and RCY408-4b (**a** *DAP1 CAN1 RAD5*) and the *DAP1*-HA derivatives RCY408-1b (**a** *DAP1*::3HA-*KanMX CAN1 RAD5*) and RCY408-5b (α *DAP1*::3HA-*KanMX CAN1 RAD5*). The two former strains were mated to produce the wild-type diploid RCY410, and the two latter strains produced the *DAP1*-HA diploid RCY411, which were used for immunofluorescence. For Erg11-Myc staining, RCY411 was transformed with pRH7 (8), which encodes Erg11 fused to a single Myc epitope tag. All genetic manipulations were performed using standard conditions.

Plasmids—The plasmid pJM63, encoding *HEM1*, was prepared by amplifying the entire *HEM1* gene using the primers *HEM1*-300F-*Bam* and *HEM1*+1722R-*Eco* and subcloning the product into the plasmid YEp*lac*195. Similarly, *HEM2* was amplified with the primers *HEM2*-300F-*Hind* and *HEM2*+1028R-*Eco* and subcloned into YEp*lac*195, forming the plasmid pJM64. For *NSG1* overexpression, the entire *NSG1* gene was amplified using the primers *NSG1*-300F and *NSG1*+873R-Myc and was initially subcloned into the PCR cloning plasmid pCR2.1, forming the plasmid pJM76. The *NSG1* fragment was the liberated as a XhoI-BamHI fragment and subcloned into the SalI and BamHI sites of YEp*lac*195, forming the plasmid pJM77.

FET3 Promoter Assays—The *FET3-lacZ* plasmid, consisting of the *FET3* promoter fused to *lacZ* in the plasmid YEp354, was the kind gift of Dr. Jerry Kaplan and has been described previously (27). For *lacZ* measurement, cells were grown in synthetic medium, with or without 100 μM bathophenanthroline disulfonic acid (BPS) for 3 h. The A_{600} was measured, and the cells were centrifuged and lysed with 250 μl of the Y-PER solution (Pierce), and the lysate was incubated with 700 μl of Z buffer (60 mM Na_2HPO_4-$7H_2O$, 40 mM NaH_2PO_4-H_2O, 10 mM KCl, 1 mM $MgSO_4$, and 50 mM β-mercaptoethanol) containing 1 mg/ml *o*-nitrophenyl β-D-galactopyranoside. The reaction was stopped with 500 μl of 1 M Na_2CO_3, clarified by centrifugation, and measured at 420 nm, using the same concentrations of Y-PER, Z buffer, and Na_2CO_3 as a blank. Miller units (($A_{420} \times 1000$)/(A_{600}/min/ml)) were calculated for each point. *FET3* transcription was assayed independently by reverse transcription-PCR as described previously (8) with the *FET3* primers *FET3*+100F (ACAGGAACGTTGATGGGCTA) and *FET3*+380R (GAATGGTACCAGTAGGTGCC). Primers for the *SCS2* transcript (8) served as a control for loading and were included in the same reaction as for *FET3*, and the products were separated in 2% agarose. Assays for ferric reductase activity were performed as described previously (28).

Protein Analysis—Log phase yeast cultures were lysed in Y-PER lysis solution (Pierce) containing 1 mM phenylmethylsulfonyl fluoride and 10 μg/ml aprotinin and analyzed essentially as described (8). The antibody to HA (HA11) was from BabCo, and the antibody to α-tubulin was developed by J. Frankel and was obtained from the Developmental Studies Bank at the University of Iowa under the auspices of the NICHD, National Institutes of Health.

For cell fractionation, cell fractions were separated by sucrose gradient essentially as described (29). Briefly, 500 ml of log phase cells were arrested with the addition of 10 mM sodium azide, chilled on ice water, and then centrifuged at 4000 × *g* for 10 min. Cells were resuspended in spheroplasting buffer (1 M sorbitol, 100 mM Tris, pH 7.8, 10 mM EDTA, and 0.3 mg/ml zymolase) and incubated at 30 °C for 40 min. Spheroplasts were

[2] The abbreviations used are: YPD, yeast-peptone-dextrose; HA, hemagglutinin; MOPS, 4-morpholinepropanesulfonic acid; BPS, bathophenanthroline disulfonic acid; MMS, methyl methanesulfonate.

then centrifuged at 700 × *g* for 10 min and resuspended in 5 ml of lysis buffer (0.8 M sorbitol, 10 mM MOPS, pH 7.2, and 1 mM EGTA) containing 1 mM phenylmethylsulfonyl fluoride. The cells were then lysed with three 10-s pulses from a Polytron PT1200 homogenizer, and the homogenate was centrifuged at 2500 × *g* for 10 min to remove unlysed cells. One ml of the lysate was separated on a discontinuous 12–60% sucrose gradient by centrifugation at 100,000 × *g* for 16 h. at 4 °C. Fractions were collected and analyzed by Western blot using antibodies to the peroxisome marker Ypt7 (a kind gift from Dr. William Wickner), the mitochondrial marker Por1 (Molecular Probes), the lipid particle marker Erg6 (a kind gift from Dr. Gunther Daum), the endosomal marker Pep12 (Molecular Probes), the plasma membrane ATPase Pma1 (a kind gift from Dr. Ramon Serrano), and Erg11 (8).

Fluorescence—Staining was performed largely as described (29). Log phase diploid cells were fixed with 3.7% formaldehyde at 37 °C for 30 min, centrifuged, resuspended in 1 M sorbitol containing 3.7% formaldehyde, and rotated at 4 °C overnight. Cells were spheroplasted in 1 M sorbitol containing 10 μg/ml zymolase and 70 mM β-mercaptoethanol at 30 °C for 1 h, washed once in PBS, and applied to a poly-L-lysine-coated slide. Cells were then permeabilized with ice-cold methanol, blocked with phosphate-buffered saline containing 1 mg/ml bovine serum albumin, and stained with the HA11 monoclonal antibody (BabCo) for Dap1-HA and an anti-Myc tag antibody (Genscript) for Erg11-Myc, followed by fluorescein isothiocyanate-conjugated secondary antibodies. For FM4–64 staining, cells were incubated with 20 μM FM4–64 (Molecular Probes) in YPD medium for 10 min, washed, and incubated for an additional 10 min in YPD before microscopic analysis. In all cases, cells were examined using a Zeiss microscope, and images were captured using Axioskop software.

Sterol Analysis—200 ml of early log phase cells were grown in YPD medium and treated with 100 μM BPS for 3 h. Cells were pelleted and washed once with distilled water and extracted with potassium hydroxide-ethanol. Sterols were subsequently extracted with hexane, as described previously (4, 8), and analyzed by gas chromatography at the University of Kentucky Mass Spectrometry Facility.

RESULTS

Strains Lacking Dap1 Are Sensitive to Iron Depletion—Wild-type and *dap1*Δ strains were maintained on iron-depleted medium by culturing in 100 μM BPS. Wild-type cells grew normally, whereas the *dap1*Δ strains did not (Fig. 1*A*, columns 3 and 4). A small zone of residual growth in the *dap1*Δ strain was dark red and consisted of nonbudded cells with a disrupted morphology. The BPS sensitivity of *dap1*Δ cells was complemented by the wild-type *DAP1* gene (Fig. 1*B*, *row 7*) but not by the *DAP1*-D91G mutant (Fig. 1*B*, *row 8*), which does not bind to heme (8). The results suggest that the heme binding function of Dap1 is required for growth under iron-depleted conditions.

The expression of the multicopper oxidase Fet3 is induced under iron-depleted conditions (30). A construct containing the *FET3* promoter fused to the bacterial *lacZ* gene was used to measure *FET3* expression. *FET3* increased 22-fold in wild-type cells and 31-fold in *dap1*Δ cells following iron depletion (Fig. 1*C*), a difference that was statistically significant ($p = 5 \times 10^{-6}$, two-tailed *t* test). The difference in *FET3* transcription in BPS-treated wild-type and *dap1*Δ cells was confirmed using using reverse transcription-PCR, where we reproducibly detected a 25% increase in *FET3* levels (Fig. 1*D*). Despite increased *FET3* transcription, we did not detect any change in the uptake of radiolabeled iron or iron reductase activity (50.5 ± 2.8 nmol of Fe^{2+}/min/A_{600} for wild type *versus* 52.6 ± 5.0 for *dap1*Δ). The results suggest a disparity between iron-regulated transcription and iron uptake in *dap1*Δ cells.

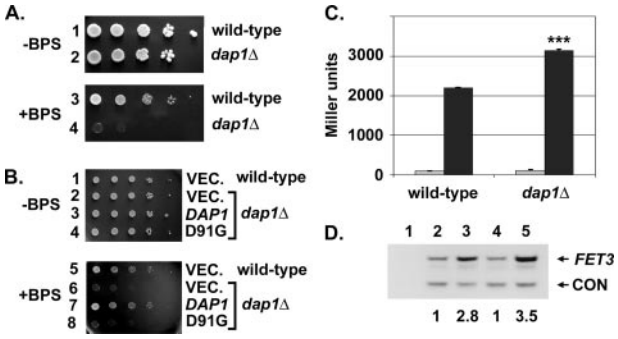

FIGURE 1. **Dap1 is required for growth under iron-depleted conditions.** *A*, wild-type (RCY409-2a) or *dap1*Δ (RCY409-4b) cells were serially diluted 1:10 and tested for viability on normal growth medium (*rows 1* and *2*) or the same medium containing 100 μM BPS, an iron-chelating agent. The *dap1*Δ strain grew poorly, and the residual colonies exhibited a dark red color. *B*, wild-type cells harboring a control vector (*rows 1* and *5*) or *dap1*Δ cells harboring the control plasmid pRS313 (*rows 2* and *6*), the *DAP1* expression plasmid pRC41 (*rows 3* and *7*), or the *DAP1*-D91G expression plasmid pRC39 (*rows 4* and *8*) were tested for growth on control medium (*rows 1–4*) or medium containing BPS (*rows 5–8*). *DAP1*-D91G encodes a point mutant of Dap1 that is incapable of binding to heme. The wild-type *DAP1* gene complemented the *dap1*Δ mutation, whereas the *DAP1*-D91G mutant did not, demonstrating a requirement for heme binding for growth on BPS. *C*, Dap1 suppresses the expression of iron-regulated genes. Wild-type or *dap1*Δ cells harboring a *FET3-lacZ* construct were untreated (*light gray columns*) or were treated with 100 μM BPS (*dark gray columns*), and β-galactosidase activity was determined in triplicate. *Error bars*, the S.D. between individual measurements. *D*, *FET3* transcripts analyzed by reverse transcription-PCR in which wild-type cells (*lanes 2* and *3*) or *dap1*Δ cells (*lanes 4* and *5*) were untreated (*lanes 2* and *4*) or treated with 100 μM BPS (*lanes 3* and *5*) for 3 h. Primers directed to the *SCS2* transcript, which is not regulated by iron, were included as an internal control for cDNA loading (*lower band*, labeled *CON* for "control"), and *lane 1* is a negative control in which the RNA template from the sample in *lane 2* was amplified without added reverse transcriptase. The *numbers below* each *lane* indicate the *FET3*/control ratio relative to the untreated wild-type cells in *lane 2*. For each assay, the results shown represent experiments that were performed at least in triplicate.

Because Dap1 regulates sterol synthesis, we tested the effect of the Dap1 mutation on sterol biosynthesis under low iron conditions. As expected, *dap1*Δ cells had elevated lanosterol and episterol relative to wild-type cells (Fig. 2, compare *A* and *C*). Treatment of wild-type cells with BPS caused a modest accumulation of episterol (Fig. 2*B*), whereas *dap1*Δ cells accumulated increased levels of squalene (Fig. 2*D*), suggesting an iron-related defect in Erg1 function in *dap1*Δ cells. The sterol synthetic pathway is diagrammed in Fig. 2*E*. Although the Erg1 substrate was elevated under iron-depleted conditions, multicopy expression of Erg1 did not suppress BPS sensitivity in *dap1*Δ cells (Fig. 2*F*, *bottom*, compare *bottom rows*), indicating that altered Erg1 function is not directly related to iron metabolic defects in *dap1*Δ cells.

Erg11 Suppresses the Requirement for Dap1 in Iron Metabolism—Because Dap1 requires heme binding for sterol synthesis, damage resistance, and viability in low iron, we devel-

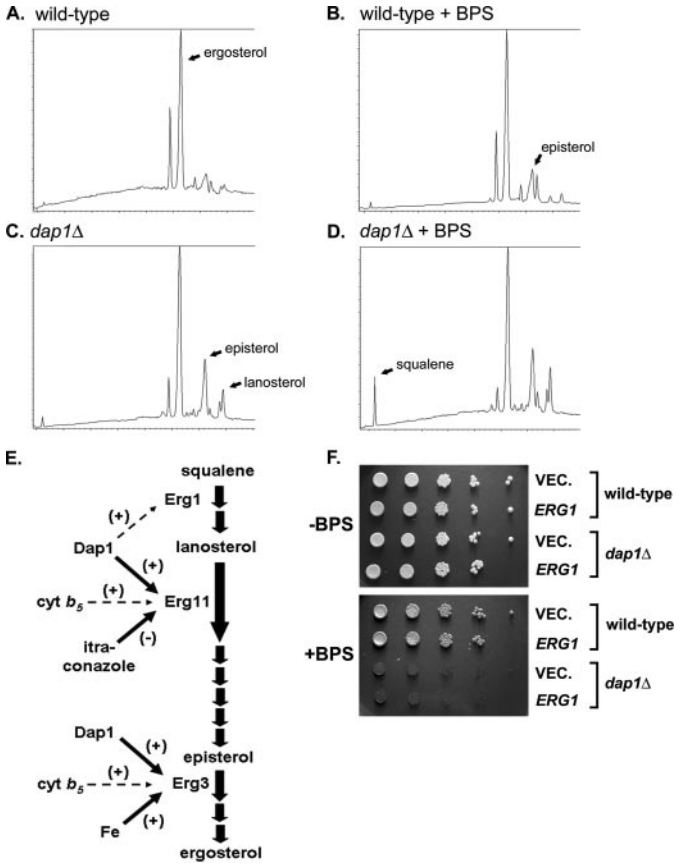

FIGURE 2. **Effect of iron deprivation on sterol synthesis.** Wild-type (RCY409-2a) (*A* and *B*) and *dap1*Δ (RCY409-4b) (*C* and *D*) were untreated (*A* and *C*) or were treated with 100 μM BPS for 3 h (*B* and *D*). Sterols were extracted and analyzed by gas chromatography. In wild-type cells, iron depletion led to a modest increase in episterol levels, whereas cells lacking Dap1 had elevated levels of episterol and lanosterol, as published previously (4), and iron depletion led to a further accumulation of squalene. *E*, the sterol biosynthetic pathway is *diagrammed*, showing the positions of the sterol intermediates that are *highlighted* in *A–D*, as well as the relevant activators and inhibitors. *F*, wild-type and *dap1*Δ cells containing a control multicopy plasmid or a multicopy plasmid harboring *ERG1* were tested for growth on control medium (*top*) or medium containing BPS (*bottom*). High copy expression of *ERG1* did not suppress iron sensitivity in *dap1*Δ cells.

oped a genetic system for increasing heme levels. The *HEM1*/δ-aminolevulinate synthase and *HEM2*/δ-aminolevulinate dehydratase genes were expressed at high copy numbers using the multiple copy plasmid YEp*lac*195, and this suppressed the elevated susceptibility of *dap1*Δ cells to the alkylating agent methyl methanesulfonate (MMS) (Fig. 3*A*). The effect was more pronounced for *HEM2* than *HEM1* (Fig. 3*A*, *rows 11* and *12*). However, *HEM1* and *HEM2* high copy expression did not suppress itraconazole sensitivity, suggesting that the expression of these genes is not limiting for sterol synthesis (Fig. 3*A*, *rows 17* and *18*). Nsg1 is the yeast homologue of the human Insig-1 protein, which binds to the human Dap1 homologue (31). However, a high dosage of *NSG1* did not suppress MMS, itraconazole, or BPS susceptibility in *dap1*Δ cells (data not shown).

Although the heme-binding domain of Dap1 was required for MMS resistance, high dose expression of *HEM2* did not suppress BPS sensitivity in *dap1*Δ cells (Fig. 3*B*, *row 11*). In contrast, high dosage of *ERG11* completely suppressed BPS sensitivity (Fig. 3*B*, *row 12*). This effect was not generalized to other sterol biosynthetic genes, because high dosage of *ERG1* and *ERG5* had no effect on BPS sensitivity in *dap1*Δ strains (data not shown). Dap1 binds to heme and is related to cytochrome b_5, encoded by *CYB5* in *S. cerevisiae*, but high copy expression of *CYB5* did not suppress loss of Dap1 (data not shown).

Because *ERG11* suppressed loss of *DAP1*, we tested the extent to which Erg11 inhibitors affected growth on iron-depleted medium. We detected partial growth of wild-type cells on 2 μM itraconazole and 100 μM BPS (Fig. 3*C*, *rows 2* and *3*, respectively) but essentially no growth when the two compounds were combined (Fig. 3*C*, *row 4*). Taken together, the results suggest that sterol synthesis mediated by Erg11 and Dap1 is required for survival in iron-depleted medium, and this Dap1 function is not a general property of cytochrome-like proteins.

Characterization of Dap1—We fused three copies of the HA epitope tag sequence through one-step integration to the 3′ end of the *DAP1* gene. As a result, *DAP1* was transcribed from its own promoter and synthesized from a single copy of its gene. The tagged Dap1 protein was readily detected as a 25-kDa protein by Western blot (Fig. 4*A*, *top*, *lanes 2* and *3*). In contrast, strains lacking the in frame epitope tag did not have a detectable 27-kDa protein (Fig. 4*A*, *top*, *lane 1*). Thus, the migration of Dap1 was similar to that of related rat and human proteins. In all cases, blots were probed with an antibody to tubulin as a control for protein loading (Fig. 4*A*, *bottom*).

Dap1 expression was reported previously to change upon treatment with the antifungal triazole drug itraconazole (7), and *dap1*Δ mutants are sensitive to itraconazole (4, 8). The expression of Dap1 increased 14-fold in cells treated with 0.1–1 μM itraconazole in a dose-dependent manner (Fig. 4*B*). In contrast, Dap1 expression did not change significantly following treatment with MMS, heat shock, or hydroxyurea (supplemental Fig. 2*A*). In addition, we did not detect any changes in Dap1 expression following treatment with BPS (supplemental Fig. 2*B*) or in strains with elongated or shortened telomeres (*tel1*Δ or *rif1*Δ *rif2*Δ, respectively; supplemental Fig. 2*C*) or in strains with acute damage sensitivity (*mec1-21*, *rad9*Δ, or *dun1*Δ).

Dap1 Localizes to Punctate Cytoplasmic Sites and Co-fractionates with Endosomal Markers—A diploid strain expressing the tagged Dap1 protein (Fig. 4*A*, *lane 4*), which was not expressed in the control untagged diploid strain (Fig. 4*A*, *top*, *lane 5*) was stained by immunofluorescence with the HA antibody. Dap1 localized to bright, clearly defined spots within the cytoplasm (Fig. 4*C*; bright field in Fig. 4*D*). The spots varied in size and number between the cells and were detectable in both mother and daughter cells. There was no evidence for Dap1 staining within the mother-bud neck, within the nucleus, or at the cell periphery. In contrast, the control diploid strain did not stain with the HA antibody after the same procedure (Fig. 4*E*; bright field shown in Fig. 4*F*). Similar spots of Dap1 staining were detected in haploid strains but were more difficult to visualize due to the smaller cell size.

Punctate cytoplasmic staining is characteristic of several types of subcellular structures. Thus, the subcellular fractions of a Dap1-tagged strain were separated on a sucrose gradient

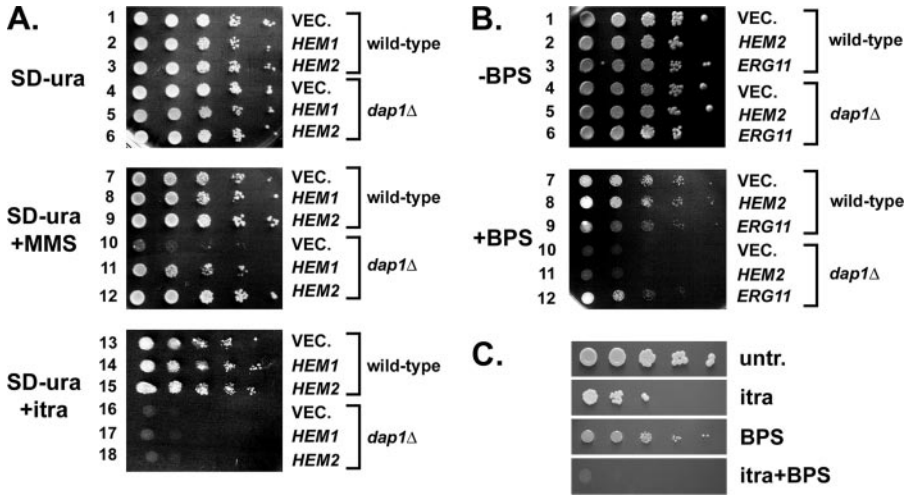

FIGURE 3. **MMS resistance is maintained by a Dap1-mediated pathway that is distinct from resistance to azole antifungal drugs and BPS.** *A*, wild-type and *dap1*Δ cells harboring the control vector YEp*lac*195 (*VEC*), a multicopy expression plasmid encoding *HEM1* (pJM63), or a multicopy expression plasmid encoding *HEM2* (pJM64) were tested for growth on synthetic dextrose (*SD*) medium lacking uracil (*rows 1–6*) or the same medium containing 0.015% MMS (*rows 7–12*) or 10 μM itraconazole (*rows 13–18*). High copy expression of *HEM1* and *HEM2* suppressed the susceptibility of *dap1*Δ cells to MMS but not itraconazole. *B*, wild-type (*rows 1–3* and *7–9*) and *dap1*Δ (*rows 4–6* and *10–12*) cells harboring the control vector YEp*lac*195 or multicopy plasmids encoding *HEM2* (pJM64) or *ERG11* (pRH4) were tested for growth on synthetic dextrose medium lacking uracil (*rows 1–6*) or the same medium containing 100 μg/ml BPS (*rows 7–12*). High level Erg11 expression suppressed loss of Dap1, whereas Hem2 did not. *C*, an azole Erg11 inhibitor increases susceptibility to BPS. Wild-type RCY409-2a were serially diluted and tested for growth on YPD plates containing 2 μM itraconazole (*row 2*), 100 μM BPS (*row 3*), or the two compounds combined (*row 4*).

and probed for Dap1 or various markers. Dap1 co-fractionated with Ypt7 (Fig. 5, *A* and *B*), a GTP-binding protein that regulates vacuolar transport (32), indicating that Dap1 co-localizes with endosomal proteins. Dap1 also partially co-fractionated with Pep12, a Q_A-type SNARE/syntaxin (33) that is a marker for late endosomes (Fig. 5*C*). In contrast, Dap1 did not co-fractionate with Erg6/sterol C-24 methyltransferase, a marker for lipid particles (Fig. 5*D*) (34, 35) or with Por1/porin, a voltage-gated anion channel and marker for mitochondria (Fig. 5*E*). The finding that Dap1 did not co-fractionate with Erg6 is consistent with an earlier mass spectrometric analysis of abundant proteins in purified lipid particles, which did not identify Dap1 (34, 36).

Mass proteomic screens for interacting proteins have identified the plasma membrane ATPase Pma1 as a putative Dap1-binding protein (37). However, our gradient detected Pma1 in a distinct portion of the gradient from Dap1 (Fig. 5*F*). Dap1 interacts genetically with Erg11 and stabilizes Erg11 expression (8). Erg11 localization was diffuse throughout the sucrose gradient (Fig. 5*G*), and Erg11 staining by immunofluorescence was granular and excluded from the vacuole (Fig. 5*H*). Previous studies with GFP-tagged Erg11 derivatives localized Erg11 to the endoplasmic reticulum (38), cytoplasm (35), or granular sites (39).

Ypt7 is related to the mammalian Rab7 protein and regulates the movement of proteins from the prevacuolar compartment to the vacuole (32). We tested the role of Dap1 in vacuolar structure by incubating wild-type and *dap1*Δ cells with the fluorescent dye FM4-64, which is internalized and stains the yeast vacuole (40). In wild-type cells, vacuoles stained as circular structures (Fig. 6*C*; the bright field image is shown in Fig. 6*A*), whereas in *dap1*Δ cells, a significant fraction of vacuoles consisted of multiple smaller structures that resembled unfused vesicles (Fig. 6*D*), and others contained irregular edges or a central septum. The color version of this figure is supplemental Fig. 3. The percentage of cells with aberrant vacuoles was elevated in *dap1*Δ cells (23 ± 5%) compared with wild type (7 ± 3%) to a significant extent (p = 0.006, two-tailed t test).

Defective vacuolar structure could inhibit vacuolar iron storage. In wild-type cells harboring a *CCC1* (cross-complements Ca^{2+} phenotype of csg1 (41); *csg* is an abbreviation for calcium-sensitive growth) high copy plasmid, *FET3-lacZ* reporter activity was highly induced (Fig. 6*E*), most likely due to iron being sequestered in the vacuole. In *dap1*Δ cells harboring the same *CCC1* plasmid, *FET3-lacZ* activity was diminished by 40% (Fig. 6*E*), a significant difference (p = 0.011, two-tailed t test). Decreased *FET3* transcription in *CCC1*-expressing *dap1*Δ cells was almost identical when *FET3* transcripts were assayed using an independent PCR technique (Fig. 6*F*, compare *lanes 3* and *5*). We detected a 38% decrease in *FET3* transcripts in *dap1*Δ cells expressing *CCC1* compared with comparable wild-type cells when calculated from the *FET3*/control transcript ratios (shown at the *bottom* of Fig. 6*F*). In triplicate analyses, the difference in *FET3* levels between *CCC1*-overexpressing wild-type and *dap1*Δ cells was statistically significant (p = 0.02, two-tailed t test). This finding is consistent with a diminished ability of *CCC1* to direct iron storage in *dap1*Δ cells. We note that the *CCC1* high copy plasmid did not affect growth of *dap1*Δ cells under low iron conditions, consistent with an additional defect in iron uptake.

DISCUSSION

Iron utilization in fungi is important clinically because the availability of free iron limits the growth of pathogenic yeast. In *dap1*Δ cells depleted of iron, *ERG11* activity is inhibited, causing toxic levels of lanosterol to accumulate. This effect is reversed by *ERG11* overexpression but not by elevated heme. It is unclear why iron depletion is toxic to cells containing elevated levels of lanosterol. One potential explanation is that the pathway that detoxifies lanosterol requires iron. Thus, deletion of *DAP1* increases lanosterol levels, and iron depletion increases its toxicity (*diagrammed* in Fig. 7). This model is supported by our finding that BPS increases susceptibility to azole drugs and by similar findings in *C. albicans* (42).

In cells lacking Dap1, iron deprivation triggers increased induction of *FET3* expression, but increased *FET3* levels do not lead to increased iron uptake or iron reductase activity, suggesting that the sterol imbalance in *dap1*Δ cells interferes with iron uptake. The model that sterol synthesis promotes iron metabolism is consistent with the findings of Li and Kaplan, in which

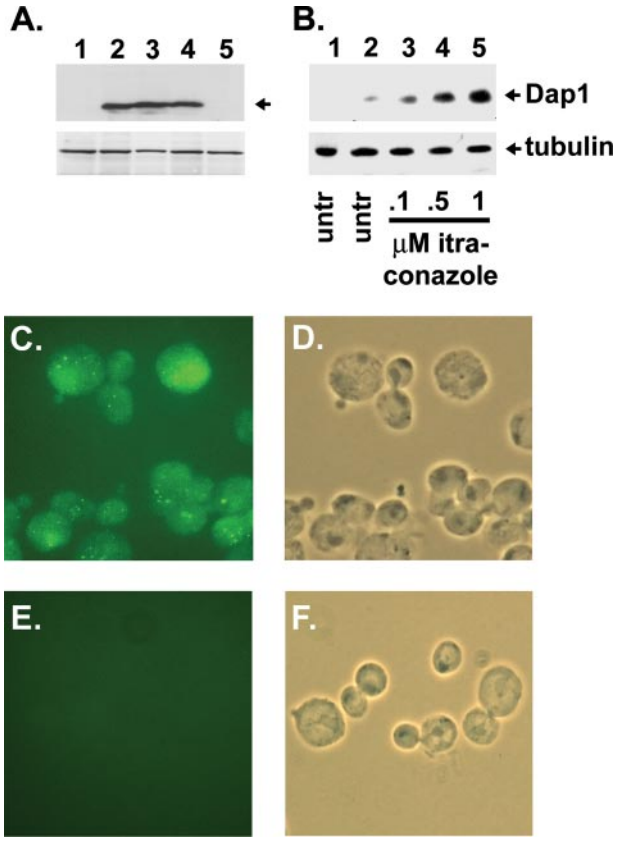

FIGURE 4. **Dap1 is induced by azole antifungal drugs.** *A*, three HA epitope tag sequences were integrated at the 3′ end of the *DAP1* open reading frame. Dap1 was detected by Western blot in haploid and diploid strains. *Lanes 1* contained the untagged haploid strain RCY408-1d, whereas *lanes 2* and *3* contained the epitope-tagged strains RCY408-1b and RCY408-5b, respectively. Two untagged strains were mated to yield the strain RCY410 (*lane 5*), whereas the epitope-tagged strains in *lanes 2* and *3* were mated to yield the diploid strain RCY411 (*lane 4*). HA-tagged Dap1 was detected as a 27 kDa band only in the strains containing the epitope-tagged *DAP1* alleles. A parallel Western blot of the same samples was probed with an antibody to tubulin as a loading control (*bottom*). *B*, Dap1 is induced by itraconazole. No Dap1 was detected in the untagged strain RCY408-1d (*lane 1*). The Dap1-HA-expressing strain RCY408-1b was untreated (*untr*) (*lane 2*) or treated with 0.1, 0.5, or 1 μM itraconazole for 90 min, and extracts were analyzed by Western blot for HA (*top*) or tubulin (*bottom*). Dap1 expression increased 14-fold relative to tubulin following itraconazole treatment. *C–F*, Dap1 localizes to punctate sites in the cytoplasm. Diploid cells expressing Dap1-HA (*C* and *D*) or untagged Dap1 (*E* and *F*) were stained with an anti-HA antibody and detected with a fluorescein isothiocyanate-labeled secondary antibody. Cells were visualized by fluorescence (*C* and *E*) or bright field microscopy (*D* and *F*). *C*, Dap1 localized to bright cytoplasmic spots. *E*, in the RCY410 strain, containing the native, untagged *DAP1* gene, punctate cytoplasmic staining was not detected. The strains RCY410 and RCY411 differed only by the HA epitope tag cassette adjacent to *DAP1* and were stained at the same time using the same conditions. The punctate staining pattern observed for RCY411 was detected in at least five separate experiments.

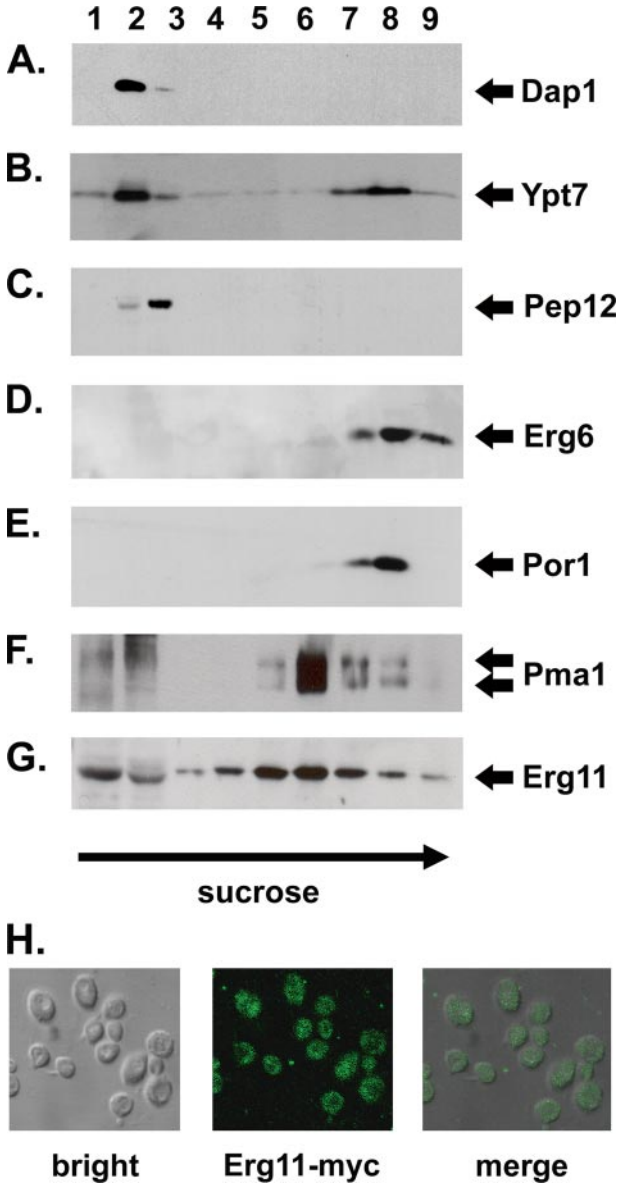

FIGURE 5. **Dap1 does not co-fractionate with mitochondrial or lipid particle markers.** RCY411 cells were lysed and separated on a 0–60% discontinuous sucrose gradient, and fractions from the gradient were collected and analyzed by Western blot. *A*, HA-tagged Dap1 was detected in fraction 2, which overlapped with the late endosomal marker Ypt7 (*B*) and partially overlapped with the late endosomal marker Pep12 (*C*). The lipid particle protein Erg6 was detected in fractions 7–9 (*D*), whereas the mitochondrial marker Por1 (*E*) was detected in fractions 7 and 8. *F*, the putative Dap1-interacting protein Pma1 localized to fraction 6. *G*, the Erg11 protein, a target of Dap1, localized in multiple subcellular fractions and overlapped partially with Dap1. *H*, in immunofluorescence studies, Erg11 was fused to a single Myc epitope tag sequence and expressed from the plasmid pRH7 in the diploid strain RCY411 and showed a granular staining pattern.

a mutation in *ERG25*/sterol C-5 methyloxidase causes sensitivity to low iron (43). However, it is unlikely that *dap1*Δ cells are sensitive to low iron solely because of low levels of ergosterol. Because conditions that have a modest effect on ergosterol levels (*i.e.* overexpression of *ERG11*) can suppress low iron sensitivity in *dap1*Δ mutants, it is likely that the balance of sterol intermediates affects iron metabolism rather than ergosterol levels *per se*.

Deletion of *DAP1* causes accumulation of the sterol intermediates lanosterol (the Erg11 substrate) and episterol (the Erg3 substrate) and of the sterol ergosta-5,7-dienol (4). Lanosterol accumulation can be suppressed by overexpressing *ERG11*, which restores azole resistance to *dap1*Δ mutants and triggers a marked accumulation of episterol and ergosta-5,7-dienol (8). Episterol presumably accumulates because Dap1 is required for the activity of Erg3/sterol C-5 desaturase (Fig. 7) (44), which is a highly conserved protein that is activated by cytochrome b_5 (6, 45), with which Dap1 shares structural homology and heme binding activity. In addition, Erg3 is also proposed to bind to iron through a series of coordinated histidine residues (43, 46),

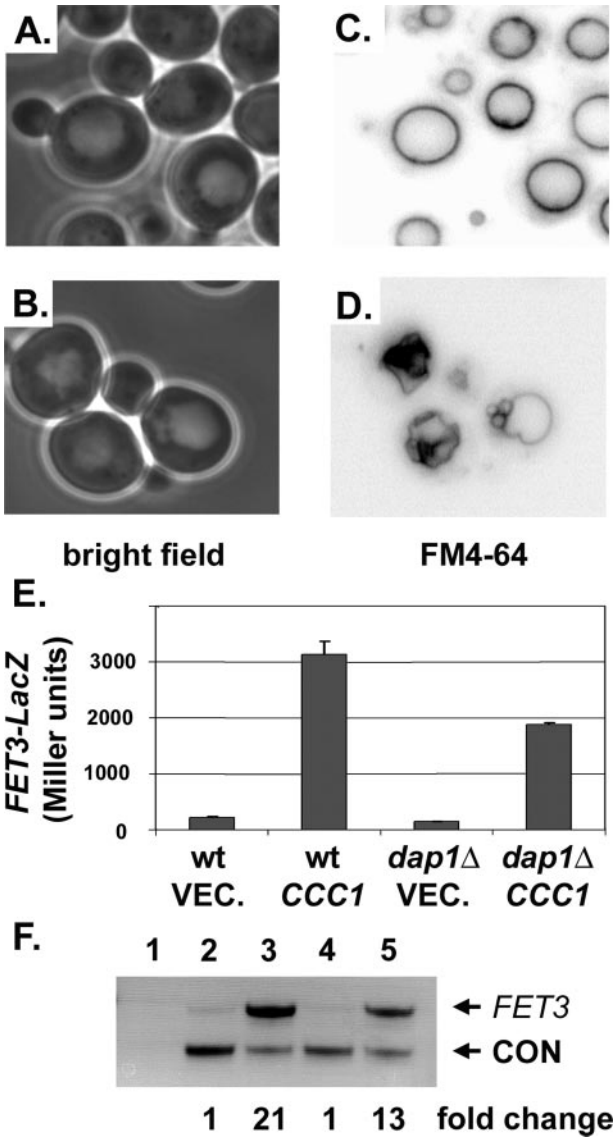

FIGURE 6. **Cells lacking Dap1 have vacuolar phenotypes.** Wild-type RCY409-2a cells (*A* and *C*) and *dap1*Δ RCY409-4b cells (*B* and *D*) were incubated with the fluorescent dye FM4-64, which stains the vacuolar membrane, and analyzed by bright field microscopy (*A* and *B*) or fluorescent microscopy (*C* and *D*). The inverted images of *C* and *D* are shown for improved contrast. In wild-type cells, vacuoles stained as round shapes, whereas a significant number of *dap1*Δ cells exhibited irregular vacuoles, including multiple smaller vacuoles. *E*, wild-type (*wt*) (RCY409-2a) or *dap1*Δ (RCY456) cells harboring a control plasmid, YEp*lac*181 (*VEC.*), or the *CCC1* high copy plasmid pSCCC1 (*CCC1*) and a *FET3-lacZ* reporter construct were tested for β-galactosidase activity. High copy *CCC1* expression increased β-galactosidase activity in wild-type cells, with a 40% decrease in *CCC1*-directed activity in *dap1*Δ cells. *Error bars*, S.D. between individual measurements. *F*, *FET3* transcription was assayed by reverse transcription-PCR in wild-type (RCY409-2a) or *dap1*Δ (RCY456) cells harboring a control plasmid, YEp*lac*181, or the *CCC1* high copy plasmid pSCCC1. Primers for the *SCS2* transcript were included in the same reaction (the product is the *lower band*) and served as a loading control (marked *CON*). The changes in the *FET3*/CON ratio relative to *lane 2* are shown *below* the gel. *Lane 1*, a control for *lane 3*, in which reverse transcriptase was omitted from the cDNA synthesis reaction. All of the assays were performed at least in triplicate.

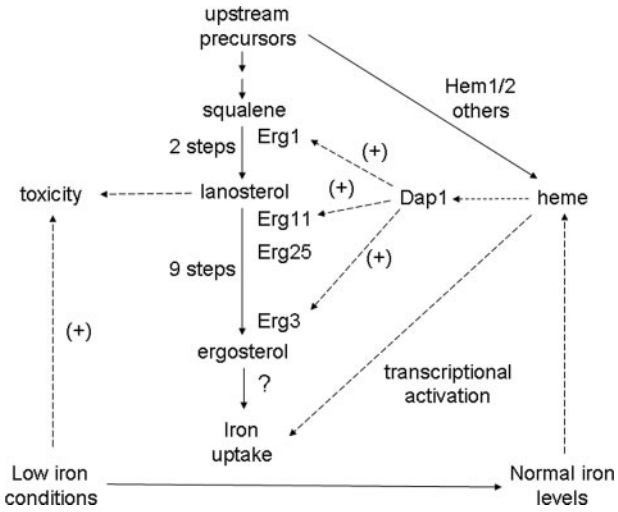

FIGURE 7. **A model in which Dap1 regulates heme and ergosterol synthesis and iron metabolism.** Iron is imported into the cell and is incorporated into heme, among other molecules. Dap1 binds to heme from its endosomal locale and activates Erg11 and Erg3, promoting sterol synthesis. Erg11 catalyzes the demethylation of lanosterol, an essential step in ergosterol synthesis, and some of the downstream metabolites of Erg11 are also detected in endosomes. Erg1 is also activated by Dap1 under low iron conditions. Our results do not exclude the possibility that iron plays a role in detoxifying sterol intermediates that accumulate in cells lacking wild-type Erg11 function (*dashed line*, *left*). There are a number of regulatory interactions between heme, the sterol pathway, and the uptake of iron, and these are not indicated.

and its substrate accumulates slightly under conditions of low iron (Fig. 2). It is intriguing to speculate that altered iron metabolism in *dap1*Δ cells may inhibit Erg3. One potential clue to the activation of Erg3 by Dap1 is that treatment of *dap1*Δ cells with heme suppresses lanosterol accumulation (*i.e.* activates Erg11) but has little effect on episterol accumulation (8), suggesting a nonheme role for activating Erg3.

Under low iron conditions, *dap1*Δ cells accumulate squalene, suggesting a defect in Erg1/squalene epoxidase. Erg1 is an oxygen-requiring enzyme that is inhibited by the allylamine class of antifungal drugs (1). Although squalene was one of the primary sterols to accumulate in iron-deprived *dap1*Δ cells, overexpression of *ERG1* did not restore viability to *dap1*Δ cells under low iron conditions, suggesting that defective Erg1 activity is not solely responsible for their defective growth.

The common target of Dap1 and its homologues is P450 protein activation, and this activity is shared among the *S. cerevisiae*, *S. pombe* (9), and rodent (12) Dap1 homologues. Mammalian Dap1 homologues are highly expressed in the liver, kidney, and adrenal, which are sites of P450 activity (10, 47, 48), and mammalian Dap1 homologues localize to microsomal fractions, including the endoplasmic reticulum (49, 50), which are also common sites for P450 proteins. The exception to this rule is in neuronal cells, where some mammalian Dap1 homologues also localize to the cell membrane (51, 52). Both the *S. pombe* Dap1 and human PGRMC1 bind directly to Cyp51 and other P450 proteins (9). In contrast, we have not detected a stable interaction between Dap1 and Erg11 in *S. cerevisiae*, and our analysis suggests only a partial overlap in their localization. Furthermore, Dap1-Erg11 complexes have not been detected using genome-wide proteomic screens or two-hybrid analyses. *S. cerevisiae* Dap1 differs from its mammalian and *S. pombe* homologues in that it lacks a membrane-spanning sequence, and it is possible that this sequence is required for a stable interaction with Erg11.

Based on the model proposed above, Dap1 probably regulates vacuolar structure via sterol synthesis. Ergosterol is nec-

essary for vacuole formation (53–56), and yeast microsomes contain a significant fraction of the sterols fecosterol, episterol, and ergosta-5,7,9(11),22-tetraenol (57–59). Our results suggest a model in which the apparent vacuolar defects in *dap1*Δ cells limit the extent to which *CCC1* sequesters iron in the vacuole. *CCC1* is postulated to act as an ion transporter, and *CCC1* overexpression triggers increased cellular iron uptake (24) and vacuolar iron storage (60). These functions are partially dependent on Dap1, although the mechanism linking these proteins is unknown.

The localization of Dap1 to intracellular vesicles and the broad distribution of Erg11 suggest that some steps in P450 activation and sterol synthesis are distributed throughout the cell. Indeed, green fluorescent protein-tagged forms of Erg2, Erg3, and Erg25 all localize to a vesicle fraction (35). Furthermore, Dap1 has been previously implicated in endocytosis (4), and the localization of Dap1 to an endosomal fraction suggests a role in intracellular transport. Although most sterol-defective mutants are hyperpermeable to dyes (61), *dap1*Δ mutants have defective dye uptake, particularly at low temperatures (4), suggesting that Dap1 is required for the endocytosis of some compounds (4). In addition, *dap1*Δ cells do not display abnormalities in membrane integrity (4) that are typical of *erg* mutants (61). The model in Fig. 7 is based on the assumption that the primary role of Dap1 is in sterol synthesis, although it is possible that Dap1 contributes to endosome function or vacuole structure through other, uncharacterized mechanisms.

Although heme is required for sterol synthesis, our results suggest that heme levels are not limiting for azole drug resistance but are limiting for MMS resistance. In contrast, we found that iron levels are limiting for azole drug resistance. Although the presumed target for MMS is DNA, Lum *et al.* (62) previously identified *HEM1* and *HEM2* in a screen for MMS targets using a genome-wide pool of heterozygous deletion strains. One interpretation of these findings is that MMS targets Hem1 and/or Hem2 directly. However, MMS sensitivity in *HEM1/hem1* and *HEM2/hem2* strains could also arise from diminished heme levels due to haploinsufficiency of 5-aminolevulinate synthase and δ-aminolevulinate dehydratase, respectively. The results are important, because MMS closely resembles chemotherapeutic drugs that are used clinically, and our results suggest a role for heme biosynthesis in susceptibility to chemotherapeutic drugs. Indeed, the human Dap1 homologue Hpr6/PGRMC1 is overexpressed in clinical tumors and cancer cell lines (50), and inhibition of Hpr6/PGRMC1 causes increased susceptibility to chemotherapeutic drugs (13).

Iron deficiency is the most prevalent nutritional disorder in the world, affecting almost two billion people (63), and abnormal iron metabolism contributes to a number of diseases, including Friedrich's ataxia, hemochromatosis, aging, and microbial infections (64). Dap1 has homologues in pathogenic fungi, including *Candida* species, and our results suggest that Dap1 homologues may have a role in iron metabolism in those organisms. If so, Dap1 homologues may be useful as targets for therapeutics, particularly in combination with other antifungal agents or under conditions leading to deprivation of available iron. There are also Dap1 homologues in higher eukaryotic species, including mammals (10, 47, 65), and the rodent and human Dap1 homologues bind to heme (12). However, the role of these proteins in iron metabolism has not been examined.

Acknowledgments—We are grateful to Gerard Crudden for expert technical assistance; to Jack Goodman for expertise in gas chromatography and mass spectrophotometry; to Martin Bard for helpful discussions; to Gunther Daum, William Wickner, and Ramon Serrano for reagents; and to Jerry Kaplan for reagents and advice about iron transport proteins.

REFERENCES

1. Daum, G., Lees, N. D., Bard, M., and Dickson, R. (1998) *Yeast* **14,** 1471–1510
2. Lepesheva, G. I., and Waterman, M. R. (2007) *Biochim. Biophys. Acta* **1770,** 467–477
3. Hannemann, F., Bichet, A., Ewen, K. M., and Bernhardt, R. (2007) *Biochim. Biophys. Acta* **1770,** 330–344
4. Hand, R. A., Jia, N., Bard, M., and Craven, R. J. (2003) *Eukaryot. Cell* **2,** 306–317
5. Mifsud, W., and Bateman, A. (2002) *Genome Biol.* **3,** 1–5
6. Schenkman, J. B., and Jansson, I. (2003) *Pharmacol. Ther.* **97,** 139–152
7. Hughes, T. R., Marton, M. J., Jones, A. R., Roberts, C. J., Stoughton, R., Armour, C. D., Bennett, H. A., Coffey, E., Dai, H., He, Y. D., Kidd, M. J., King, A. M., Meyer, M. R., Slade, D., Lum, P. Y., Stepaniants, S. B., Shoemaker, D. D., Gachotte, D., Chakraburtty, K., Simon, J., Bard, M., and Friend, S. H. (2000) *Cell* **102,** 109–126
8. Mallory, J. C., Crudden, G., Johnson, B. L., Mo, C., Pierson, C. A., Bard, M., and Craven, R. J. (2005) *Mol. Cell Biol.* **25,** 1669–1679
9. Hughes, A. L., Powell, D. W., Bard, M., Eckstein, J., Barbuch, R., Link, A. J., and Espenshade, P. J. (2007) *Cell Metab.* **5,** 143–149
10. Gerdes, D., Wehling, M., Leube, B., and Falkenstein, E. (1998) *Biol. Chem.* **379,** 907–911
11. Ghosh, K., Thompson, A. M., Goldbeck, R. A., Shi, X., Whitman, S., Oh, E., Zhiwu, Z., Vulpe, C., and Holman, T. R. (2005) *Biochemistry* **44,** 16729–16736
12. Min, L., Takemori, H., Nonaka, Y., Katoh, Y., Doi, J., Horike, N., Osamu, H., Raza, F. S., Vinson, G. P., and Okamoto, M. (2004) *Mol. Cell Endocrinol.* **215,** 143–148
13. Crudden, G., Chitti, R. E., and Craven, R. J. (2006) *J. Pharmacol. Exp. Ther.* **316,** 448–455
14. Mense, S. M., and Zhang, L. (2006) *Cell Res.* **16,** 681–692
15. Weinstein, J. D., Branchaud, R., Beale, S. I., Bement, W. J., and Sinclair, P. R. (1986) *Arch. Biochem. Biophys.* **245,** 44–50
16. Guarente, L., Lalonde, B., Gifford, P., and Alani, E. (1984) *Cell* **36,** 503–511
17. Zhang, L., and Hach, A. (1999) *Cell Mol. Life Sci.* **56,** 415–426
18. Crisp, R. J., Pollington, A., Galea, C., Jaron, S., Yamaguchi-Iwai, Y., and Kaplan, J. (2003) *J. Biol. Chem.* **278,** 45499–45506
19. Puig, S., Askeland, E., and Thiele, D. J. (2005) *Cell* **120,** 99–110
20. Shakoury-Elizeh, M., Tiedeman, J., Rashford, J., Ferea, T., Demeter, J., Garcia, E., Rolfes, R., Brown, P. O., Botstein, D., and Philpott, C. C. (2004) *Mol. Biol. Cell* **15,** 1233–1243
21. Felice, M. R., De Domenico, I., Li, L., Ward, D. M., Bartok, B., Musci, G., and Kaplan, J. (2005) *J. Biol. Chem.* **280,** 22181–22190
22. Thomas, B. J., and Rothstein, R. (1989) *Cell* **56,** 619–630
23. Craven, R. J., and Petes, T. D. (2001) *Genetics* **158,** 145–154
24. Chen, O. S., and Kaplan, J. (2000) *J. Biol. Chem.* **275,** 7626–7632
25. Longtine, M. S., McKenzie, A., 3rd, Demarini, D. J., Shah, N. G., Wach, A., Brachat, A., Philippsen, P., and Pringle, J. R. (1998) *Yeast* **14,** 953–961
26. Craven, R. J., Greenwell, P. W., Dominska, M., and Petes, T. D. (2002) *Genetics* **161,** 493–507
27. Li, L., and Kaplan, J. (2001) *J. Biol. Chem.* **276,** 5036–5043
28. Dancis, A., Klausner, R. D., Hinnebusch, A. G., and Barriocanal, J. G. (1990) *Mol. Cell Biol.* **10,** 2294–2301
29. Kagiwada, S., Hosaka, K., Murata, M., Nikawa, J., and Takatsuki, A. (1998)

J. Bacteriol. **180,** 1700–1708
30. Van Ho, A., Ward, D. M., and Kaplan, J. (2002) *Annu. Rev. Microbiol.* **56,** 237–261
31. Suchanek, M., Radzikowska, A., and Thiele, C. (2005) *Nat. Methods* **2,** 261–267
32. Wichmann, H., Hengst, L., and Gallwitz, D. (1992) *Cell* **71,** 1131–1142
33. Bowers, K., and Stevens, T. H. (2005) *Biochim. Biophys. Acta* **1744,** 438–454
34. Zweytick, D., Athenstaedt, K., and Daum, G. (2000) *Biochim. Biophys. Acta* **1469,** 101–120
35. Natter, K., Leitner, P., Faschinger, A., Wolinski, H., McCraith, S., Fields, S., and Kohlwein, S. D. (2005) *Mol. Cell Proteomics* **4,** 662–672
36. Athenstaedt, K., Zweytick, D., Jandrositz, A., Kohlwein, S. D., and Daum, G. (1999) *J. Bacteriol.* **181,** 6441–6448
37. Ho, Y., Gruhler, A., Heilbut, A., Bader, G. D., Moore, L., Adams, S. L., Millar, A., Taylor, P., Bennett, K., Boutilier, K., Yang, L., Wolting, C., Donaldson, I., Schandorff, S., Shewnarane, J., Vo, M., Taggart, J., Goudreault, M., Muskat, B., Alfarano, C., Dewar, D., Lin, Z., Michalickova, K., Willems, A. R., Sassi, H., Nielsen, P. A., Rasmussen, K. J., Andersen, J. R., Johansen, L. E., Hansen, L. H., Jespersen, H., Podtelejnikov, A., Nielsen, E., Crawford, J., Poulsen, V., Sorensen, B. D., Matthiesen, J., Hendrickson, R. C., Gleeson, F., Pawson, T., Moran, M. F., Durocher, D., Mann, M., Hogue, C. W., Figeys, D., and Tyers, M. (2002) *Nature* **415,** 180–183
38. Huh, W. K., Falvo, J. V., Gerke, L. C., Carroll, A. S., Howson, R. W., Weissman, J. S., and O'Shea, E. K. (2003) *Nature* **425,** 686–691
39. Wiwatwattana, N., Landau, C. M., Cope, G. J., Harp, G. A., and Kumar, A. (2007) *Nucleic Acids Res.* **35,** 810–814
40. Vida, T. A., and Emr, S. D. (1995) *J. Cell Biol.* **128,** 779–792
41. Fu, D., Beeler, T., and Dunn, T. (1994) *Yeast* **10,** 515–521
42. Prasad, T., Chandra, A., Mukhopadhyay, C. K., and Prasad, R. (2006) *Antimicrob. Agents Chemother.* **50,** 3597–3606
43. Li, L., and Kaplan, J. (1996) *J. Biol. Chem.* **271,** 16927–16933
44. Arthington, B. A., Bennett, L. G., Skatrud, P. L., Guynn, C. J., Barbuch, R. J., Ulbright, C. E., and Bard, M. (1991) *Gene* (*Amst.*) **102,** 39–44
45. Reddy, V. V., Kupfer, D., and Caspi, E. (1977) *J. Biol. Chem.* **252,** 2797–2801
46. Rahier, A., Benveniste, P., Husselstein, T., and Taton, M. (2000) *Biochem. Soc. Trans.* **28,** 799–803
47. Selmin, O., Lucier, G. W., Clark, G. C., Tritscher, A. M., Vanden Heuvel, J. P., Gastel, J. A., Walker, N. J., Sutter, T. R., and Bell, D. A. (1996) *Carcinogenesis* **17,** 2609–2615
48. Raza, F. S., Takemori, H., Tojo, H., Okamoto, M., and Vinson, G. P. (2001) *Eur. J. Biochem.* **268,** 2141–2147
49. Nolte, I., Jeckel, D., Wieland, F. T., and Sohn, K. (2000) *Biochim. Biophys. Acta* **1543,** 123–130
50. Crudden, G., Loesel, R., and Craven, R. J. (2005) *Tumour Biol.* **26,** 142–146
51. Labombarda, F., Gonzalez, S. L., Deniselle, M. C., Vinson, G. P., Schumacher, M., De Nicola, A. F., and Guennoun, R. (2003) *J. Neurochem.* **87,** 902–913
52. Krebs, C. J., Jarvis, E. D., Chan, J., Lydon, J. P., Ogawa, S., and Pfaff, D. W. (2000) *Proc. Natl. Acad. Sci. U. S. A.* **97,** 12816–12821
53. Fratti, R. A., Jun, Y., Merz, A. J., Margolis, N., and Wickner, W. (2004) *J. Cell Biol.* **167,** 1087–1098
54. Souza, C. M., and Pichler, H. (2007) *Biochim. Biophys. Acta* **1771,** 442–454
55. Kato, M., and Wickner, W. (2001) *EMBO J.* **20,** 4035–4040
56. Seeley, E. S., Kato, M., Margolis, N., Wickner, W., and Eitzen, G. (2002) *Mol. Biol. Cell* **13,** 782–794
57. Zinser, E., Paltauf, F., and Daum, G. (1993) *J. Bacteriol.* **175,** 2853–2858
58. Zinser, E., Sperka-Gottlieb, C. D., Fasch, E. V., Kohlwein, S. D., Paltauf, F., and Daum, G. (1991) *J. Bacteriol.* **173,** 2026–2034
59. Gaspar, M. L., Aregullin, M. A., Jesch, S. A., Nunez, L. R., Villa-Garcia, M., and Henry, S. A. (2007) *Biochim. Biophys. Acta* **1771,** 241–254
60. Li, L., Chen, O. S., McVey Ward, D., and Kaplan, J. (2001) *J. Biol. Chem.* **276,** 29515–29519
61. Gaber, R. F., Copple, D. M., Kennedy, B. K., Vidal, M., and Bard, M. (1989) *Mol. Cell Biol.* **9,** 3447–3456
62. Lum, P. Y., Armour, C. D., Stepaniants, S. B., Cavet, G., Wolf, M. K., Butler, J. S., Hinshaw, J. C., Garnier, P., Prestwich, G. D., Leonardson, A., Garrett-Engele, P., Rush, C. M., Bard, M., Schimmack, G., Phillips, J. W., Roberts, C. J., and Shoemaker, D. D. (2004) *Cell* **116,** 121–137
63. Baynes, R. D., and Bothwell, T. H. (1990) *Annu. Rev. Nutr.* **10,** 133–148
64. Roy, C. N., and Andrews, N. C. (2001) *Hum. Mol. Genet.* **10,** 2181–2186
65. Falkenstein, E., Meyer, C., Eisen, C., Scriba, P. C., and Wehling, M. (1996) *Biochem. Biophys. Res. Commun.* **229,** 86–89